We thank the referees for their review, comments and suggestions. We have found these comments to be very useful and we have implemented all of them in the revised manuscript and/ or addressed them here in direct reply section. We feel that the paper has been significantly improved by making these changes. The text also has received polishing several times. The major changes in this new revision are: (I) In the result section, we have magnified a 10 seconds window when the events happen to present a better detail about the dynamics of the turbine responses. (II) A reproducibility section has been added which investigate the similarity of the wind velocity profiles in this study compare to the previous study (**Shirzadeh, K., Hangan, H. and Crawford, C.: Experimental and numerical simulation of extreme operational conditions for horizontal axis wind turbines based on the IEC standard, Wind Energy Science, 5(4), 1755–1770, doi:10.5194/wes-5-1755-2020, 2020**.) that shows the current setup reproduces the same events.

We address below each of your comments. At the end of this file the marked-up manuscript with highlighted changes is attached. The location of the corresponding changes is mentioned in each answer to comment.

RC1

Abstract

- L11: add the corresponding parameter to the length, radius or diameter.

  Ans: diameter has been added.

- L11-13: It seems that the two sentences were together before, the second one does not sustain itself.

  Ans: they have been rearranged

- L16: the TSR was not studying to state that. Moreover, is this not always the case?

  Ans: Correct, that sentence has been excluded.

1.Introduction

- L20-30: note that the word energy is used nine times during these two paragraphs.
  Ans: different set of words have been used, thank you.
- L32: the number “2” should be written with letters according to the standard of the Journal, this type of corrections go throughout all the paper (equation -> Eq, figure -> Fig, etc.), you can take a look in the submission settings (https://www.wind-energyscience. net/submission.html
  Ans: corrections have been considered,
- L41: First person is used only a couple of times during the text (we L41, our L42, our L121), like the rest of the manuscript does not, this should be changed.
  Ans: corrections have been made

- L47: please check the use of blade's and blades' throughout the manuscript.
  Ans: corrections have been made
- L72: This statement is regarding this setup? L42 says that there is a previous work.
  Ans: That sentence has been deleted. The same setup has been used in this study. new set of words have been used.
- L76-79: This is a sentence for the methodology.
  Ans: to prevent redundancy it has been removed.

2. **Deterministic EOC**

- L93: please number both equations.
  Ans: it has been added.
- L113: This is unclear. TSR is by definition a function of freestream, rotational speed and radius, so the length scale is only a function of TSR, using the same argument. Is it possible to show this similarity approach by additional equations?
  Ans: The scaling is function of (I) free stream velocity, (II) rotor rotational speed or TSR, (III) rotor size. The corresponding equation has been added. (equation 8)
- L120: The inflow was just represented by the theoretical profiles and four probes position? This is critical for the study, the gusts were performed several times to study reproducibility?
  Ans: Here the inflow is just presented with the four probes. But in the previous study seven probes in a vertical or horizontal array, depending on the extreme event, were used. Their locations were based on the turbine rotor dimension, two out of the seven probes (probes B & H) were at similar height or lateral distance to the probes in this study. Based on this, a reproducibility analysis has been added just for the flow field. In previous study reproducibility analysis have not been performed, because it included a long process of trial and error for flow modulation and data processing. Therefore, in this study a complementary reproducibility analysis has been added in section 4.3
- L122: What are the consequences of this?
  Ans: more description has been added in line 135. "This simplification stretches the actual rising and falling time, yet, this is the compromise that was made due to hardware limitations. For a wind turbine that operates in a specific average wind, it is the velocity excursion above the average wind speed that is important to capture. More detailed information about the scaling method and the EOCs flow fields are accessible in (Shirzadeh et al., 2020)."
- L126: ..that these extreme "operational condition" models . However, they Provide
  Ans: changes have been made, line 142, Thank you.
- L129: are there more realistic approaches?
  Ans: by simple we mean symmetric and totally deterministic. As far as we know these are the guidelines that are being used by designers and manufacturers. Even though the new version of the standard (2019) uses statistical approach for prescribing the peak factors the generic shapes are still the same.

3.Experimental methodology

- L131: The homogeneity of the flow is missing, were the measurements (normal and events) done more than once?
  Ans: A transitioning sentence has been added. Line 146. The experiments were done once for each event. "As mentioned earlier, in this study similar inflow fields with the ones developed in (Shirzadeh et al., 2020) were reproduced to investigate

the responses of the wind turbine to these scaled transient conditions. For each extreme event only one measurement run was performed. The reproducibility of these events was ensured by direct comparison with the previous study."

- L141: please provide the specific downstream location.
  Ans: more details have been added. Line 160
- L142: Please consider the word opening instead of open to avoid the open-close confusion.

Ans: this has been considered, thank you.

- L146: change filed by field.

Ans: it has been fixed.

- L147: What does mean 1.3m from the centerline of the primary flow direction?

Ans: The lateral distance from the center or offset from the center. Different wording has been used. Line 169.

- L148: It is the case? How are the probes in relation to the fan positioning? Was the inflow studied with more probes?

Ans: The flow has been studied in more details in the previous study. For this study we used four probes around the rotor just to see when exactly the event happens in relation with the loads and power generation. This setup also help us to picture the 2D flow field over the rotor without adding more complexity to our experiment setup.

- L151: Please provide details from all the sensors.

Ans: sensor models have been added in the text about proximity sensor and the force balance. More details on Cobra probes is available in the previous study as mentioned in text, Line 174.

- L154: specifications are needed. The signal synchronization details are missing. The calibration procedures of the sensors are missing.

Ans: it all happened in the data acquisition software. Line 185. Also picture of the interface box has been added in figure 3. "analogue voltage signals cables (six voltages from force balance, one from proximity sensor and one from load terminals), plus four wind velocity signals cobra probe cables gathered to one deck, synchronized and logged at 2000 Hz frequency for 90s for each experiment run. All the signals were calibrated as zero in the Turbulent Flow data acquisition software when the 60 fans were off."

- L162-168: How is this correlation done?

Ans: By 'correlated' we meant related. Different wording has been used. line 189

- L163: the most important in terms of? (Also in L243)

Ans: line 191, in terms of magnitude and correlation with performance of the turbine.

- L168: Here is stated that the inflow has heterogeneity, how much?

Ans: this sentence states the Z moment is representing the twist in the structure, which is important in EHS event. However, when fans are uniformly operating there is a slight non-uniformity that induces 0.1 Nm steady yaw moment. Relative to the moment that the EHS induces (1.5 Nm) this is negligible.

L173: Why only part of the results are normalized? Are then the results comparable?

Ans: other parameters were close to zero. Using them to normalize the parameter would have give unreasonably large normal values.

- Table 1: is this TI calculated as the EIC description? AS this shows only the average of the four probes, how scattered are the results between probes? The axis letters are small and Figure 4 shows them in capital. As the mean values are different, the normalization is done by different values?

Ans: TI here are smaller compared to the IEC standard. Matching turbulence was not the focus of these studies. When using all the fans with contraction walls the flow characteristics are uniform. However, in creating EWS when we just used the 20 fans in the middle the flow close to the ceiling is more turbulent. More details can be found in the previous study. The axes letters have been switched to capital.

Yes, We used Case A to normalize EWSs (EVS, negative EVS, EHS) and case B to normalize EOG.

- L193: this is from only one probe?

Ans: line 223, it represents the spatial averaged (i.e. averaged from all the probes)

- L194: which frequencies?

Ans: frequencies have been added, line 225.

- L195: add dimension to the value.

Ans: dimension added.

- L195-197: this is unclear.

Ans: line 227, different wording was used.

- L204: check the comma position.

Ans: done, thanks.

- L207: Is this 0.25% over the full scale range? This needs clarification to neglect it. "The JR3 multi-axis force/ torque sensor (75E20S175E20S4-6000N) at the base of the tower has ±0.25% nominal accuracy of the measuring value for all axes".

Ans: JR3 force balances are very sensitive. Clarifications have been added. Line 239.

- L209: There are more than moving average method, which one was used? Please provide a reference.

Ans: reference has been added. Line 250.

- L211: This is unclear

Ans: based on the criteria described in (Chowdhury, J., Chowdhury, J., Parvu, D., Karami, M. and Hangan, H.: Wind flow characteristics of a model downburst, in American Society of Mechanical Engineers, Fluids Engineering Division (Publication) FEDSM, vol. 1, American Society of Mechanical Engineers (ASME)., 2018.) the moving average time window was chosen to just filter low energy fluctuations from the main signal, so if you plot these fluctuating part of the signal separately the mean value of them is zero.

- L215: Please elaborate on this.

Ans: line 254, they are essentially zero with some fluctuations.

- Table 2: Is the power epistemic uncertainty 0%? This table should include the values aforementioned in [N] and [Nm]. Clarification in what is the reference to the %. How was the combined uncertainty calculated?

Ans: the voltage signal from generator was directly connected to the interface box so essentially the only uncertainty is analog to digital conversion. Mean values of the parameters have been added to the table, clarifications have been added , line 252. Combined uncertainty calculation in line 251.

4. Results

- L221: A brief introduction on how the results are presented would improve the understanding of the following sections.

Ans: now the result subfigures have window number, introduction has been provided, line 262- 266.

- L225: normalized electrical power

Ans: changed, thank you.

- L226: starred.

Ans: changed, thank you.

- L227: Due to the normalization, as both quantities have uncertainties there is an error propagation, is this considered?

Ans: This have been neglected as now mentioned in line 254.

- L232-234: is an outlook that could go at the end of the document.

Ans: It has been moved to line 363.

- Figure 6: This can be improved by separating them into three Figures with a): : :e) subfigures. As there is no much information or analysis on the steady parts, it would be beneficial zoom in on the event. On the caption: starred. It is possible to perform a frequency spectrum analysis and decouple some influences?

Ans: four times magnified windows have been added to the figures, thank you. We have done frequency analysis for highly fluctuating X-moment to see if there are any peaks related to vortex shedding so we can filter that. There were some energy peaks but we couldn't find any relation between those frequency with vortex shedding and rotor rotation frequency. As the focus of this study is to measure the global loading and power generation we chose not to include any frequency analysis here .

- L246: is there some reference that supports the magnitude of this value?

Ans: there is a very interesting CFD simulation of a 87 m diameter turbine (Cai, X., Gu, R., Pan, P. and Zhu, J.: Unsteady aerodynamics simulation of a full-scale horizontal axis wind turbine using CFD methodology, Energy Conversion and Management, 112, 146–156, doi:https://doi.org/10.1016/j.enconman.2015.12.084, 2016.). The yaw moment in the typical yaw condition as they calculated is about 30 to 90 Nm as blades rotate. Comparisons have been added in line 300.

- L249: The first sentence should go in the methodology. The second sentence needs to be rephrased.

Ans: this has been done, thank you.

- L252: Is this the case or could be a time delay?

Ans: there is no delay in EOGs, the flow is perfectly uniform.

- L251-258: From here, it can be inferred that any electrical power data do not provide valuable information? Which is the rated condition of the turbine? Do the conclusions could change with a reduced, rated or overrated operational condition?

Ans: The nominal TSR for this turbine is 5. It is known that generators in low rotor speeds have very high hysteresis losses which can bring their efficiency as low as 20-30 %. Therefore it would have been better if we were able to directly measure the mechanical power. As it has been mentioned in the future works, more investigation in various operational TSRs needs to be performed to asses the scaling method results with what actually happens in full scale. The conclusions definitely can change with various operational TSR and actually that is one of the main points of the proposed scaling method to relate this result to a full range of full scale conditions.

- L259: How can be stated that these differences depend on the hub height and diameter if they were fixed?

Ans: We meant that Y-moment is the moment of X-force with the lever-arm close to the hub height. The sentence was not necessary and it has been deleted.

- L263: please add a reference.

Ans: this is based on our results. clarifications have been added in line 321.

- L264-267: Is this a hypothesis? Is this not contradictory with the electrical power statement on L251-258?

Ans: This is the analysis of the results. Essentially turbines in various TSR have various capabilities in extracting energy from the gust. Some part of the energy in the gust get stored in form of angular momentum with excess instantaneously transformed in power generation. After the gust, that stored momentum energy gradually transforms to power generation. As it can be seen figure 7 window II.

- L268: First sentence needs to be rewritten.

Ans: different wording has been used. Line 227.

- L274: Why they might not?

Ans: Because they may have different/stiffer structure.

5. Conclusions

- L277: add the corresponding parameter to the length, radius or diameter.

Ans: done, thank you.

- L284: No control was done in this study to state that.

Ans: correct, different wordings have been used. Line 366.

- L286: No variation of the TSR was done to conclude this.

Ans: correct, different wordings have been used. Line 368.

RC2

Section 3:

- No information about the turbine is provided. Could you provide relevant data of turbine design, blade control (collective - IPC), turbine control (fixed speed or controlled speed), operation of the turbine (is it working as a full scale turbine?) and similarity wth full scale. Is it reasonable to make these extreme loads tests with a TSR of 1.1? Is there any similarity with a full scale turbine power extraction? or blade relative wind kinematics? If hte blade is already all stalled there may not be a great sensitivity on the rotor performance.

Ans: this turbine is the exact turbine that has been examined in (Refan, M. and Hangan, H.: Aerodynamic Performance of a Small Horizontal Axis Wind Turbine, Journal of Solar Energy Engineering, 134(2), doi:10.1115/1.4005751, 2012.) it does not have any active control. "The turbine has 1 kW rated power at 12 m/s wind speed and nominal TSR of 5" line 182.

We are using a new scaling method which has been elaborated in the previous study. Supplementary explanation has been added (equation 8). The main similarity considered, is the wake kinematics compared to full scale. The blades are probably stalled in this low TSR, and you are correct, our results are dependent on the TSR. As mentioned in future works the previously proposed scaling method needs further investigation.

- Line 147 - typo: filed –> field

Ans: changed, thank you.

- Line 156 - The total number of signals should be 12 from Cobras (u,v,w), 6 from force balance,the proximity and the load terminals.

Ans: there is a misunderstanding here, figure 3 has been re arranged to better present the setup. From each cobra probe there is one cable and it is actually the software that process the data and gives (u,v,w).

- Line 156 - how are you computing TSR? what is your reference velocity?

Ans: the averaged velocity from all the probes is the reference velocity. Clarifications have been added in Line 182. Thank you.

- Figure 3: very low quality image: could you please increase it.

Ans: it has been re arranged with new details.

- Figure 6 - it could be useful to mark on each subfigure the beginning and the end of the extreme event.

Ans: it has been re arranged, thank you.

- Line 263 - The power generation peak and decay depends on the turbine rotor control, therefore it may be useful to have more details.

Ans: as it has been mentioned in line 308, no means of control has been used. In this case based on our results the power peak happens at the end of the EOG, and its decay purely depends on rotor inertia and the amount of stored angular momentum at the end of the EOG.

Investigating the loads and performance of a model horizontal axis wind turbine under reproducible IEC extreme operational conditions

Kamran Shirzadeh [1,2], Horia Hangan [1,3], Curran Crawford [1,4], Pooyan Hashemi Tari [5]

[1] WindEEE Research Institute, University of Western Ontario, London, Ontario, N6M 0E2, Canada
[2] Mechanical and Material Engineering, Western University, London, N6A 3K7, Canada
[3] Civil and Environment Engineering, Western University, London, N6A 3K7, Canada
[4] Mechanical Engineering, Victoria University, Victoria, V8W 2Y2, Canada
[5] Mechanical Engineering, Shahid Beheshti University, Tehran, 19839 69411, Iran

Correspondence: Kamran Shirzadeh (kshirzad@uwo.ca)

Abstract. The power ~~performance~~generation and loading dynamic responses of a 2.2 m ~~scaled~~diameter horizontal axis wind turbine (HAWT) under some of the IEC 61400-1 transient extreme operational ~~extreme~~ conditions ~~were investigated. Extreme~~, more specifically, extreme wind shears (EWS) and extreme operational gust (EOG) ~~inflow conditions, generated in~~ that were reproduced at the WindEEE ~~dome~~Dome at Western University~~. were investigated~~. The global forces were measured by a multi axis force balance at the HAWT tower base. The unsteady horizontal shear induced a significant yaw moment on the rotor with a similar dynamic ~~loads~~ as the extreme event ~~with no serious effect on~~without effecting the power generation. The EOG severely affected all the performance parameters of the turbine ~~which were highly dependent on the operational TSR and the time duration of the event~~.

Keywords: Extreme operational Gust; Extreme Shear; HAWT; IEC Standard; Wind Tunnel; Transient Experiment.

1. Introduction

In the past two decades, wind energy has grown to become one of the primary sources of energy being installed worldwide in an effort to reduce greenhouse gas emissions. One of the main factors of this increasing trend is the continued decreasing price of ~~energy~~electricity generated by wind energy devices. It is still expected for this market to grow by having even lower levelized cost of electricity (LCOE) in the near future (McKinsey & Company, 2019). This price reduction can be facilitated by more technological advancements (e.g. building larger rotors) and better understanding of the interaction between different wind conditions and the turbines in order to increase the life cycle of these wind energy systems.

The dynamic nature of the atmospheric boundary layers (ABL) affects all the dynamic outputs of the wind ~~energy systems~~turbines; these all bring challenges to further growth of the wind energy share in the energy sector. One of the main challenges for todays' wind ~~energy systems~~turbines are the power generation fluctuations which cause instability in the grid network (Anvari et al., 2016). It has been reported that the effect of the extreme events can get transferred to the grid with even amplification in magnitudes (amount of power generation is related to the cube of wind velocity); the power output of the

Formatted: English (Canada)
Formatted: English (Canada)
Formatted: English (Canada)
Formatted: English (Canada)
Formatted: English (Canada)
Formatted: English (Canada)
Formatted: English (Canada)
Formatted: English (Canada)
Formatted: English (Canada)
Formatted: English (Canada)
Formatted: English (Canada)
Formatted: English (Canada)
Formatted: English (Canada)
Formatted: English (Canada)
Formatted: English (Canada)
Formatted: English (Canada)
Formatted: English (Canada)
Formatted: English (Canada)
Formatted: English (Canada)

whole wind farm can change by 50% in just ~~2~~two minutes (Milan et al., 2013). These turbulent features also induce fatigue loads on the blades (Burton et al., 2011) predominantly for the flap wise loadings (Rezaeiha et al., 2017), which then get transferred to the gearbox (Feng et al., 2013), bearings and then the whole structure. Implementation of LIDAR technology can make revolutionary contribution to this matter by measuring the upstream flow field and give enough time to the control system to properly adjust itself (e.g. blade pitch angles, generator load & etc~~).~~) in order to reduce overall power fluctuations and the mechanical load variations (Bossanyi et al., 2014).

During the past few decades some comprehensive design guidelines have been developed in terms of load analysis. The International Electrotechnical Commission (IEC) included some deterministic design load cases for commercial horizontal axis wind turbines (HAWT) in operating condition in the IEC 61400-1 document (IEC, 2005) followed by statistical analysis introduced in the latest edition (IEC, 2019). ~~Herein we test the power generation and loads on a scaled HAWT for representative deterministic gust design conditions as per IEC 2005. In our previous study, (Shirzadeh et al., 2020) the development of the corresponding scaled extreme transient wind fields was carried out. More specifically, the extreme operational gust (EOG) and extreme wind shears (EWS) which includes the extreme vertical and horizontal shears (EVS and EHS), were all experimentally simulated in the WindEEE dome.~~Herein the power generation and loads on a scaled HAWT is being tested under representative deterministic gust design conditions as per IEC 2005. This is an extension to the previous study, (Shirzadeh et al., 2020) that incorporated the developments of the corresponding scaled extreme operational gust (EOG) and extreme wind shears (EWS) that includes the extreme vertical and horizontal shears (EVS and EHS), in the WindEEE Dome.

From an aerodynamic perspective the effective angle of attack on the blades and consequently the global lift and drag forces increase during wind gust conditions which result in ~~blade's~~blades' torque, thrust and root moment amplification. Several experimental studies have been conducted to control the rotor aerodynamics under these transient events. The application of the adaptive camber airfoil in a gusty inflow generated by active grid was investigated by Wester et al., 2018. These ~~type~~types of airfoils have coupled leading and trailing edge flaps, which can be adjusted to de-camber the profile with increasing lift force. This proved to reduce the integral lift force about 20% at the peak in a gust event. ~~Petrović et al., 2019~~Petrović et al., 2019 developed an algorithm for a PI controller of the pitch angles of a scaled wind turbine in the wind gust conditions generated by an active grid. Using the algorithm, they were able to reduce over speeding of the rotor and the blades' bending moments.

The effect of the wind shears on wind turbine aerodynamics has been studied by several investigators. The effect of various steady shear flows and turbulence intensities, generated by active grid, on the near wake region of a small scaled turbine was investigated by Li et al., 2020 using PIV measurements. It has been found that the absolute mean velocity deficit in this region remains symmetric and it is insensitive to the inflow non-uniformity. Also, the mean power production does not change with the amount of the shear. However, the power fluctuation has a linear correlation with the amount of background turbulence intensity, in other words, the effect of higher shears translated as a higher inflow turbulence and therefore higher fluctuations in power. Similar results were reported by Sezer-Uzol and Uzol, 2013 who used a three-dimensional unsteady vortex-panel

Formatted: English (Canada)

method to investigate the effect of transient EWS on the performance of a HAWT. They found that due to the EWS, the blades experience asymmetrical surface pressure variations. Consequently, the rotor produces power and thrust with high amplitude of fluctuations which can cause significant structural issues and reduce the lifetime of the turbine. From the field data perspective it has been reported that for the same reference wind speed, higher turbulence intensities result in relative higher power efficiencies below the nominal operational condition but the efficiency decreases in transition to rated power (Albers et al., 2007).

Mostly, transient flow fields have been previously generated either numerically or physically by means of active grids. While some of these studies ~~reproduced~~produced various transient flows, none had attempted to reproduce ~~and apply~~ the EOG and EWS as per IEC standards and ~~compare the results~~apply it on a wind turbine with ~~stationary and uniform inflow conditions~~a relevant scaling which ~~constitutes~~constitute the main objectives of the present study. ~~Moreover, the present work employs for the first time a matrix of individually controlled fans to generate customized flow fields and investigate their effect on a model scale wind turbine.~~ The work has been ~~done~~performed at the WindEEE ~~dome~~Dome at Western University Canada. Alongside with the numerical simulations and field data, this setup can contribute to fast development of the new control prototypes of HAWT for customized transient wind effects.

~~This is an experimental study for examination of the load and power generation of the turbine under four unsteady extreme condition cases (EVS, EHS, negative EVS and EOG), developed in (Shirzadeh et al., 2020). To provide an examination of changes relative to a baseline reference, the results in each case have been normalized with values from a corresponding uniform inflow.~~

The paper is organized as follows. Section 2 briefly presents the target deterministic operational extreme conditions. Section 3 details the WindEEE chamber and the experiment setups; this section also provides the details about the uniform flow fields used as reference values for comparisons. Section 4 presents the results from EWSs and EOG~~,~~ and the capability of the facility in reproducing these conditions. Section 5 is dedicated to conclusions.

2. Deterministic extreme operating conditions

Prior to introducing the deterministic gust models, it is informative to know how the standard (IEC, 2005) classifies wind turbines based on a reference wind speed and turbulence intensity (TI). The TI in the standard is given for a specific height and is defined as the ratio of the mean standard deviation of wind speed fluctuations to the mean wind speed value at that height, both calculated in 10 min intervals. Three classes of reference wind speeds (U_{ref}: I, II and III) and three classes of turbulence intensities (I_{ref}: A, B and C) are defined that gives a combination of 9 external turbine design conditions that have specified values. One further class for special conditions (e.g. off-shore and tropical storms) is considered which should be

Formatted: English (Canada)

specified by the designer. Correspondingly, ~~an~~ extreme wind speed ~~model~~models as a function of height (Z) with respect to the hub height (Z_{hub}) with recurrence period of 50 years (U_{e50}) and 1 year (U_{e1}), ~~is~~are defined as follows:

$$U_{e50}(z) = 1.4U_{ref}\left(\frac{Z}{Z_{hub}}\right)^{0.11} \quad (1)$$

$$U_{e1}(z) = 0.8U_{e50}(z) \quad (2)$$

Based on the turbulence class, the streamwise hub height velocity standard deviation (σ_u), is defined by what is called the normal turbulence model as equation (3).

$$\sigma_u = I_{ref}(0.75\overline{U_{hub}} + 5.6) \quad (3)$$

$\overline{U_{hub}}$ is the average velocity at hub height.

Based on equation ~~(1)~~(2) and (3) the hub height gust magnitude (U_{gust}) is given as:

$$U_{gust} = min\left\{1.35(U_{e1} - U_{hub}); 3.3\left(\frac{\sigma_u}{1+0.1\left(\frac{D}{\Lambda_u}\right)}\right)\right\} \quad (4)$$

Taking $t = 0$ as the beginning of the gust, the velocity time evolution of the EOG is defined as:

~~$$U(t) = \begin{cases} \overline{U_{hub}} - 0.37U_{gust}\sin\frac{3\pi t}{T}\left(1 - \cos\frac{2\pi t}{T}\right); when \quad 0 \le t \le T, \\ \overline{U_{hub}}; \quad when\ t > T\ or\ t < 0, \end{cases} U(t)$$~~

$$= \begin{cases} \overline{U_{hub}} - 0.37U_{gust}\sin\frac{3\pi t}{T}\left(1 - \cos\frac{2\pi t}{T}\right); when \quad 0 \le t \le T, \\ \overline{U_{hub}}; \quad when\ t > T\ or\ t < 0. \end{cases} \quad (5)$$

T is the duration of the EOG, specified as 10.5 seconds, D is the diameter of the rotor and Λ_u is the longitudinal turbulence scale parameter which is a function of the hub height:

~~$$\Lambda_u = \begin{cases} 0.7Z_{hub} & for\ Z_{hub} \le 60\ m, \\ 42\ m & for\ Z_{hub} > 60\ m, \end{cases} \Lambda_u$$~~

$$= \begin{cases} 0.7Z_{hub} & for\ Z_{hub} \le 60\ m, \\ 42\ m & for\ Z_{hub} > 60\ m. \end{cases} \quad (6)$$

The EWS can be added to or subtracted from the main uniform or ABL inflows. The EVS velocity time evolution at a specific height (Z) can be calculated using equation (7).

Formatted
Formatted
Formatted
Formatted
Formatted Table
Formatted
Split Cells
Formatted
Formatted
Formatted: Font: Cambria Math, Italic, English (Canada)
Formatted: English (Canada)
Formatted: English (Canada)
Formatted
Formatted
Formatted
Formatted: English (Canada)
Formatted
Formatted: English (Canada)
Formatted
Formatted
Formatted: English (Canada)
Formatted
Formatted Table
Formatted
Formatted: English (Canada)
Formatted
Formatted: English (Canada)
Formatted
Formatted: English (Canada)
Formatted
Formatted: English (Canada)
Formatted: English (Canada)
Formatted: English (Canada)
Formatted: English (Canada)
Formatted: English (Canada)

$$U_{EVS}(Z,t) = \begin{cases} \left(\frac{Z - Z_{hub}}{D}\right)\left(2.5 + 1.28\sigma_u\left(\frac{D}{\Lambda_u}\right)^{0.25}\right)\left(1 - \cos\left(\frac{2\pi t}{T}\right)\right); when \;\; 0 \le t \le T, \\ 0 \;\; ; when\; t > T \; or \; t < 0, \end{cases} U_{EVS}(Z,t)$$

$$= \begin{cases} \left(\frac{Z - Z_{hub}}{D}\right)\left(2.5 + 1.28\sigma_u\left(\frac{D}{\Lambda_u}\right)^{0.25}\right)\left(1 - \cos\left(\frac{2\pi t}{T}\right)\right); when \;\; 0 \le t \le T, \\ 0 \;\; ; when\; t > T \; or \; t < 0. \end{cases} \quad (7)$$

The EWS duration is 12 s. For a commercial IIJ_B class HAWT with 92 m diameter and 80 m tower hub height, at 10 m/s average velocity, the prescribed EOG and EVS are presented in Figure 1a & b. The time windows in these figures start and end with the extreme event. The standard gust durations in operation condition are relatively long compared to the response time of scaled wind turbines. Herein, we assume these time durations (10.5 s for EOG and 12 s for EWS) correspond to 4 complete rotor revolutions period in commercial wind turbines which typically have a rotational speed in the range of $\sim 15 - 20\ RPM$; or in another words, the gust time duration is equal to the ~~propagation~~advection of the four complete tip vortex loops from a specific blade in the wake~~.~~ by the free stream. Accordingly, the time scale becomes a function of ~~TSR~~rotor angular velocity or the tip speed ratio (i.e. TSR the ratio of the blade tip linear velocity over the free stream), free stream velocity and diameter of the rotor; ~~the length scale is just a function of TSR and diameter of the rotor. For~~for a scaled wind turbine, the duration corresponding to four revolutions in similar nominal operating conditions is in the order of one second. The experiments in the earlier study showed that the fastest possible gust obtained in the WindEEE ~~dome with the desired peak factor is around 5 seconds (Shirzadeh et al., 2020).~~Dome with the desired peak factor was around five seconds (Shirzadeh et al., 2020). Therefore, it is possible to relevantly decrease the wind speed and TSR to match up the parameters ~~up~~based on the assumption above that results in equation (8):

$$\frac{\boldsymbol{T_s} U_{hub} \lambda}{\pi D} = 4. \quad (8)$$

where $\boldsymbol{T_s}$ is the scaled time (here is 5 s) and λ is the operating TSR. Assuming a similar IIJ_B class HAWT with hub height of ~2 m with the 2.2 m diameter scaled wind turbine, at 5 m/s average hub-height velocity, the extreme condition profiles look identical to the full-scale ones (the same peak factor but different gust time) as presented in Figure 1c & d. These are the inflow fields that are considered in the present experiments. Therefore, based on ~~our~~this assumption the turbine should be working at 1.1 TSR. Also due to hardware limitation in the physical experiments, the EOG has been simplified by excluding the velocity drops before and after the main peak as it is shown in Figure 1c in red-dashed line. This simplification stretches the actual rising and falling time, yet, this is the compromise that was made due to hardware limitations. For a wind turbine that operates in a specific average wind, it is the velocity excursion above the average wind speed that is important to capture. More detailed information about the scaling method and the EOCs flow fields are accessible in (Shirzadeh et al., 2020).

Formatted Table
Formatted: English (Canada)
Formatted: English (Canada)
Formatted: English (Canada)
Formatted: English (Canada)
Formatted: English (Canada)
Formatted: English (Canada)
Formatted: English (Canada)
Formatted: English (Canada)
Formatted: English (Canada)
Formatted: English (Canada)
Formatted: English (Canada)
Formatted: English (Canada)
Formatted: English (Canada)
Formatted: English (Canada)
Formatted: Indent: First line: 0 cm
Formatted: English (Canada)
Formatted: English (Canada)
Formatted: English (Canada)
Formatted: English (Canada)
Formatted: English (Canada)
Formatted: English (Canada)
Formatted: English (Canada)
Formatted: English (Canada)
Formatted: English (Canada)
Formatted: English (Canada)

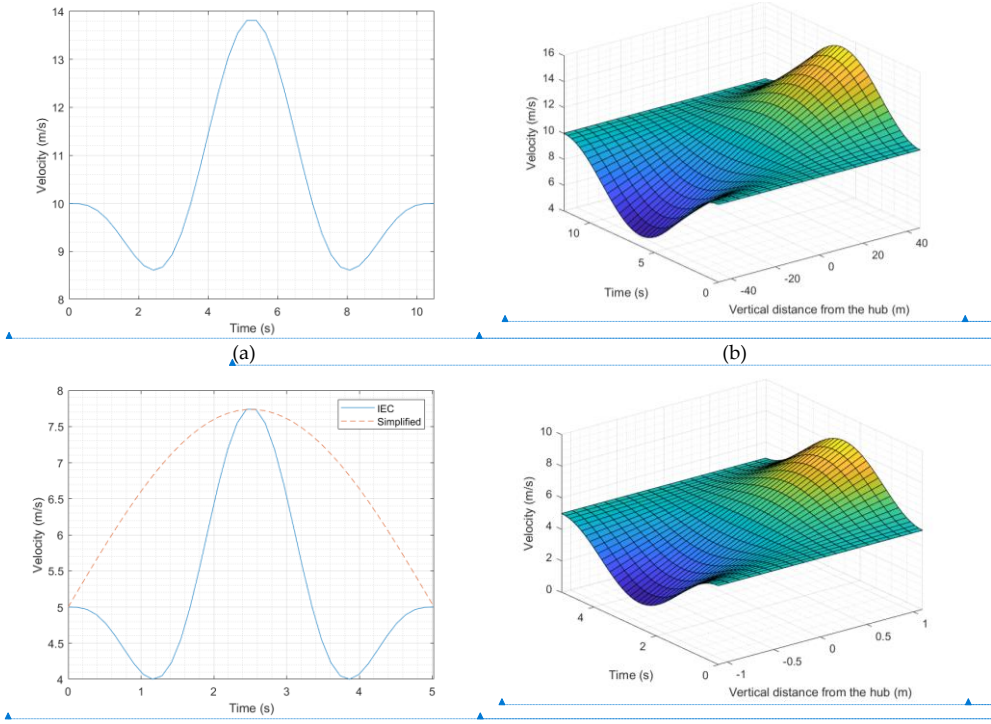

Figure 1: Extreme operational conditions for a full scale HAWT III_B class with 92m diameter and hub height of 80m at 10 m/s uniform wind speed, (a) extreme operational gust, (b) extreme vertical shear on the rotor with hub height as reference, The scaled extreme condition, (c) the IEC EOG and the simplified EOG that was targeted, (d) extreme vertical shear. ~~Adopted from (Shirzadeh et al., 2020)~~Adopted from (Shirzadeh et al., 2020).

It is worth to mention that these extreme operational condition models are relatively simple and not able to capture the real dynamics of the ABL flow-field that directly affect the performance of the turbine (Schottler et al., 2017; Wächter et al., 2012). However, ~~it provides~~they provide practical guidelines for the development and wind tunnel testing of HAWTs.

3. Experimental methodology

~~3.1. WindEEE dome~~

As mentioned earlier, in this study similar inflow fields with the ones developed in (Shirzadeh et al., 2020) were reproduced to investigate the responses of the wind turbine to these scaled transient conditions. For each extreme event only one measurement run was performed. The reproducibility of these events was ensured by direct comparison with the previous study.

3.1. WindEEE Dome

The experiments were carried out at the Wind Engineering, Energy and Environment (WindEEE) Dome at Western University, Canada. The test chamber has 25 m diameter footprint and 3.8 m height with a total number of 106 fans among which 60 fans mounted along one of the hexagonal walls in a 4×15 matrix and 40 fans are on the rest of the peripheral five walls (Figure 2a). 6 other larger fans are in a plenum above the test chamber usually being used for 3D flows like tornado and down bursts (Hangan et al., 2017). In the present study, experiments were carried out using the dome in 2D flow (e.g. ABL, uniform straight flows and etc.) closed circuit mode which just the 60-fan wall is operated. In this mode the flow recirculates from the top through the outer shell as it is shown in Figure 2a. Each of these fans are 0.8 m in diameter and are individually controlled to a percentage of their 30-kW maximum power using variable frequency drives. In order to reach higher velocities at lower fan power set-points at the test chamber for generating EOG a 2D contraction with ratio of ~~3~~three, was installed ~~just~~at the outlet of 60 fans wall that extends for 7.5 m downstream ~~of the 60-fan wall~~ (Figure 2a). These fans are equipped with adjustable inlet guiding vanes (IGV). They can be adjusted stationary from 0% ~~open~~opening (close) to 100% ~~open~~opening or dynamically in ~~a~~an open-close cycle ~~of opening and closing~~ (Figure 2b). By using this feature the ~~uniform gusts~~EOGs were produced. The ~~transient shears~~EWSs were produced by power modification of the 5 middle fan columns (20 fans). Therefore, contraction walls had no effect on the EWS flow fields.

Formatted: English (Canada)
Formatted: English (Canada)
Formatted: English (Canada)
Formatted: English (Canada)
Formatted: English (Canada)
Formatted: English (Canada)
Formatted: English (Canada)
Formatted: English (Canada)
Formatted: English (Canada)
Formatted: English (Canada)
Formatted: English (Canada)
Formatted: English (Canada)
Formatted: English (Canada)
Formatted: English (Canada)
Formatted: English (Canada)
Formatted: English (Canada)
Formatted: English (Canada)
Formatted: English (Canada)

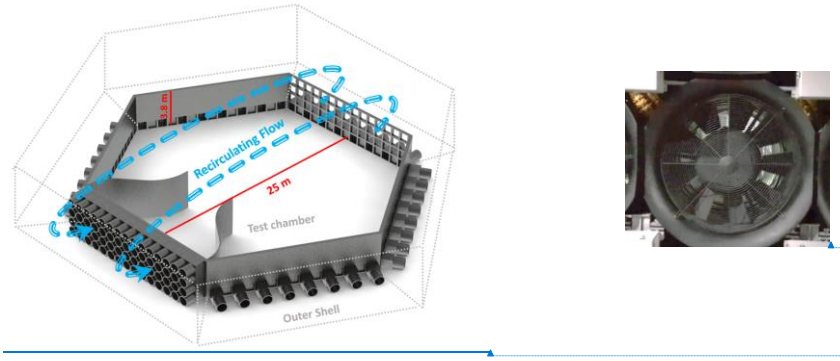

(a) (b)

Figure 2. ~~Simplified geometry of the~~ WindEEE dome, (a) the test chamber and the contraction walls with the flow recirculation path through the outer shell in closed circuit 2D flow mode, (b) ~~The~~the adjustable vanes at the inlets of the 60 fans at 70% ~~open~~opening vanes state.

3.2. Experimental setup for power and load performance

To measure the velocity of the flow ~~filed~~field, four cobra probes (TFI Ltd., 2011) are used in a plane ~~1m~~1 m upstream (~0.5 D) the rotor with 1.3 m left and right offset ~~1.3m~~ from the ~~centerline of the primary flow direction~~rotor's hub. The probes are set at 3m and 0.8m heights corresponding to the highest and lowest heights of the rotating blades' tips (Figure 3). With this configuration the cobra probes can give a proper perception of the flow field over the wind turbine rotor plane. ~~The wind turbine was mounted on a six-component force balance sensor for measuring all 3 forces/ shears and 3 moments at the base of the tower. After mounting the turbine, the force balance was calibrated as zero. In addition, a light photoelectric diffuse reflection proximity sensor~~More specific details about cobra probes are found in (Shirzadeh et al., 2020). The wind turbine was mounted on a six-component force balance sensor for measuring all 3 shear forces and 3 moments at the base of the tower. In addition, a light photoelectric diffuse reflection proximity sensor (Autonics BR200-DDTN) was used which gives a voltage pulse once it detects a light reflection from the blade passing in front. Using the pulse, one can measure the angular velocity of the rotor with a high resolution (three times a revolution). The turbine has 1 kW rated power at 12 m/s wind speed and nominal TSR of 5 (Refan and Hangan, 2012). This wind turbine is equipped with a three phase AC generator. A specific electrical circuit was used to convert the voltage and current to DC and feed the power to the resistors. The last parameter that was monitored was the voltage from the terminals of the power resistors which were set at constant 8.1Ω in order to keep the rotor at the desired TSR (= 1.1~~).~~) that has been calculated based on the averaged wind speed from all the cobra probes. At the end, eight analogue voltage ~~signals~~cables (six voltages from force balance, one from proximity sensor and one from load terminals), plus four ~~wind velocity signals~~ cobra probe cables gathered to one deck, synchronized and logged at 2000 Hz

Formatted: English (Canada)
Formatted: English (Canada)
Formatted: English (Canada)
Formatted: English (Canada)
Formatted: English (Canada)
Formatted: English (Canada)
Formatted: English (Canada)
Formatted: English (Canada)
Formatted: English (Canada)
Formatted: English (Canada)
Formatted: English (Canada)
Formatted: English (Canada)
Formatted: English (Canada)
Formatted: English (Canada)
Formatted: English (Canada)
Formatted: English (Canada)
Formatted: English (Canada)
Formatted: English (Canada)
Formatted: English (Canada)
Formatted: English (Canada)
Formatted: English (Canada)
Formatted: English (Canada)
Formatted: English (Canada)
Formatted: English (Canada)
Formatted: English (Canada)
Formatted: English (Canada)
Formatted: English (Canada)
Formatted: English (Canada)
Formatted: English (Canada)

frequency for 90s for each experiment run. All the signals were calibrated as zero in the Turbulent Flow data acquisition software when the 60 fans were off.

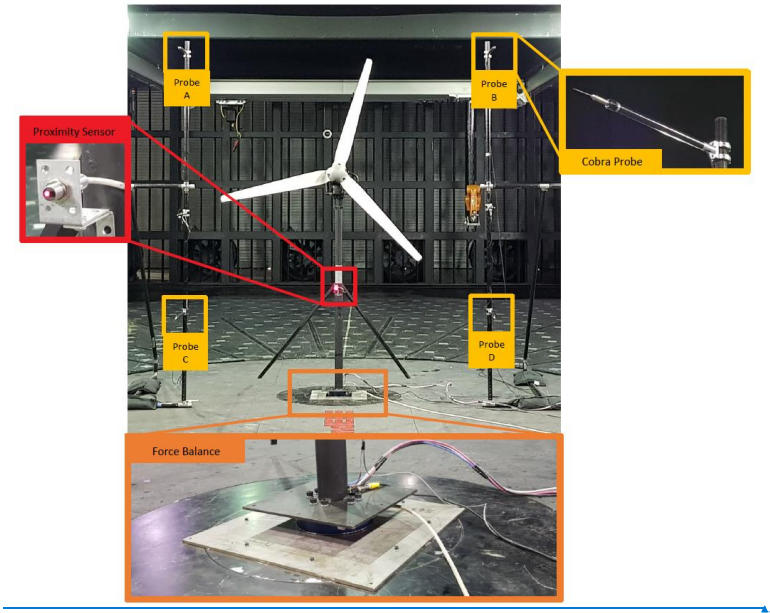

Formatted: English (Canada)

Formatted Table

Formatted: English (Canada)

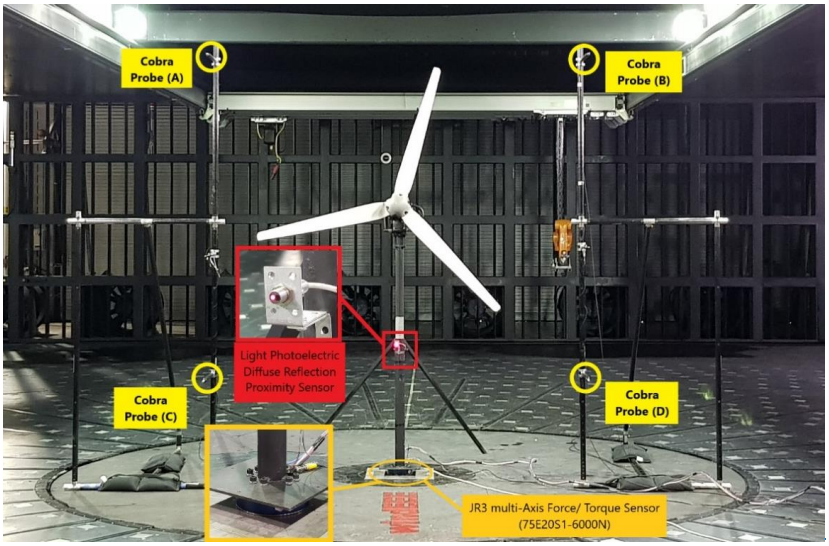
Cobra Probe (A)
Cobra Probe (B)
Light Photoelectric Diffuse Reflection Proximity Sensor
Cobra Probe (C)
Cobra Probe (D)
JR3 multi-Axis Force/ Torque Sensor (75E20S1-6000N)

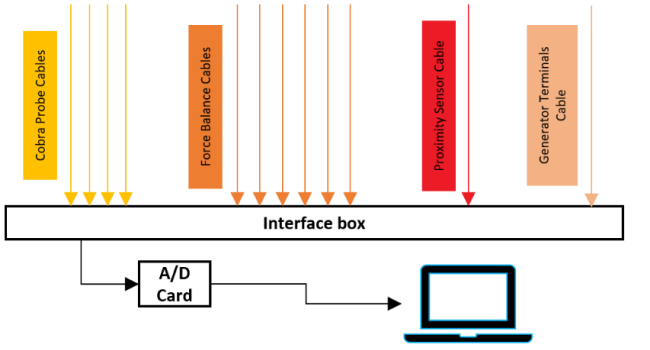
Cobra Probe Cables
Force Balance Cables
Proximity Sensor Cable
Generator Terminals Cable
Interface box
A/D Card

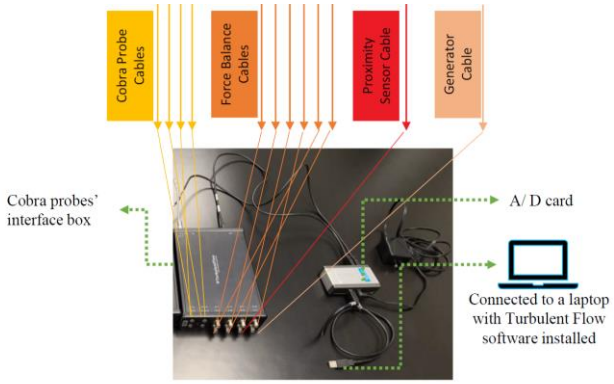

Figure 3. Setup for measuring power performance and dynamic loads for different types of inflow

The schematic of the positioning of the wind turbine and the cobra probes relative to the local coordinate system (centre of the WindEEE dome/ base of the tower) is depicted in Figure 4. ~~The shear forces and moments~~Some of the loads at the base are inherently correlated with the performance of the wind turbine. Based on this local coordinate system, the most important shear force in terms of both magnitude and correlation with turbine's performance at the base is in the X direction which represents the thrust of the rotor plus the drag force of the tower. The X moment represents torque on the generator plus induced vortex shedding moment; the Y moment shows the bending moment due to drag on the whole structure (correlated to the forces in X direction). The moment around the Z axis shows the ~~torsion~~twist due to horizontal non-uniformity of the flow. The Z force represents the lift on the structure.

Formatted: English (United Kingdom)
Formatted: English (Canada)
Formatted: English (Canada)
Formatted: English (Canada)
Formatted: English (Canada)
Formatted: English (Canada)
Formatted: English (Canada)
Formatted: English (Canada)
Formatted: English (Canada)
Formatted: English (Canada)
Formatted: English (Canada)

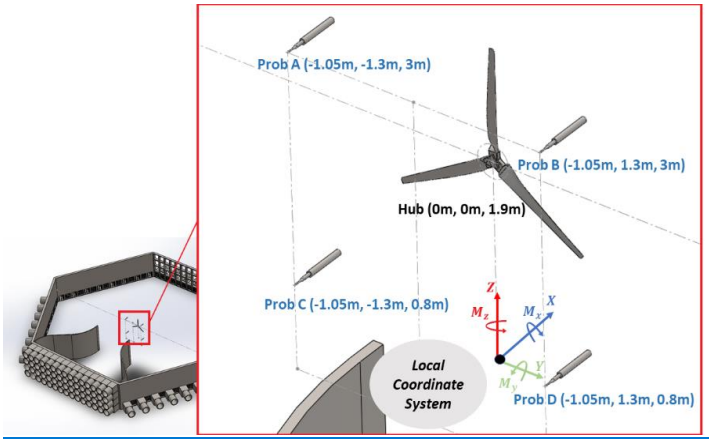

Figure 4. The arrangement of cobra probes and HAWT relative to local coordinate system

3.3. Baseline uniform inflows

As mentioned earlier, in this study four unsteady extreme condition cases (EVS, EHS, negative EVS and EOG) are considered for the investigation. For the EWSs just the 20 middle fans and in the EOG all of the fans were operated. Some of the results from power performance and loadings of each case are normalized with their corresponding averaged data from one of the two different 5 m/s steady uniform wind inflow (cases A & B in Table 1). Cases A & B were used to normalize the EWSs and the EOG respectively. The reason for using different uniform cases is due to the difference in the flow characteristics (TI and spectra) related to the different fan setups for each case. At this low TSR, considerable parts of the blades are in stall and the TI magnitude can affect the flow behavior on the suction side of the blades and result in noticeable difference in loads and power performance of the wind turbine. The mean and RMS values of the data obtained from the force balance, turbine power and TSR from these two uniform cases are tabulated in Table 1. The bolded values in this table will be used to normalize the corresponding data from the transient experiment cases. ~~Case A & B for normalizing the EWSs and the EOG respectively~~The rest of the parameters present random fluctuating values around zero and therefore they were not normalized.

Formatted: English (Canada)
Formatted: English (Canada)
Formatted: English (Canada)
Formatted: English (Canada)
Formatted: English (Canada)
Formatted: English (Canada)
Formatted: English (Canada)
Formatted: English (Canada)
Formatted: English (Canada)
Formatted: English (Canada)
Formatted: English (Canada)

Table 1. The mean values of loads and power generation in different steady uniform cases (with the same load, 8.1Ω)

5 m/s Uniform Case	Fan Configuration	Average wind velocity and TI from all the cobra probes	Turbine Performance (mean value | standard deviation)			
				~~x~~ X-axis	~~y~~ Y-axis	~~z~~ Z-axis
A	*5 columns at middle at 40% and IGVs at 100% open* 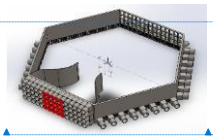	4.91 m/s, 16%	Shears (N)	**14.36** | 0.45	-0.22 | 0.37	-4.8| 0.69
			Moments (Nm)	**0.87** | 0.19	**-20.51** | 0.91	-0.14 | .25
			Electrical power (W)		**0.81**| 0.04	
			TSR		1.30 | 0.11	
B	*All fans at 30% and IGVs at 10% open* 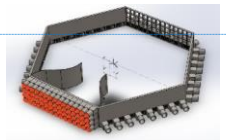	5.15 m/s, 10%		~~x~~ X-axis	~~y~~ Y-axis	~~z~~ Z-axis
			Shears (N)	**14.39** | 0.44	-0.48 | 0.32	-5.36 | 0.71
			Moments (Nm)	**0.84** | 0.16	**-23.06** | 0.92	-0.25| 0.30
			Electrical power (W)		**0.67** | 0.02	
			TSR		1.08 | 0.08	

The spatial averaged turbulence spectra ~~of~~by the four cobra probes for these two uniform cases are presented in Figure 5. There is a consistent noise from the fans with its harmonics at some specific high frequencies~~.~~ (~200 Hz and 400 Hz in case A, ~200 Hz and 600 Hz in case B). Due to the steadiness of the flow, large share of the energy is distributed at the low-end frequencies (i.e. frequencies lower than 3 Hz). In this region, the two cases show the same energy distribution. However, for frequencies higher ~~or~~and equal to ~~3Hz~~ 3 Hz or length scales of 1.65 m and smaller (based on the frozen turbulence hypothesis ~~corresponds to length scales of 1.65m and smaller ($\frac{1}{3}[s] \times 5\left[\frac{m}{s}\right] =$~~at 5 m/s average wind speed, $\frac{1}{3\ Hz} \times 5\ m/s = 1.65\ [m]$~~)~~), difference in energy distribution is noticeable with lower turbulence energy in case B in all the corresponding frequencies relative to case A. All the spectra follow the -5/3 slope consistent with the Kolmogorov theory in inertial subrange (Pope, 2000).

Formatted
Formatted
Formatted

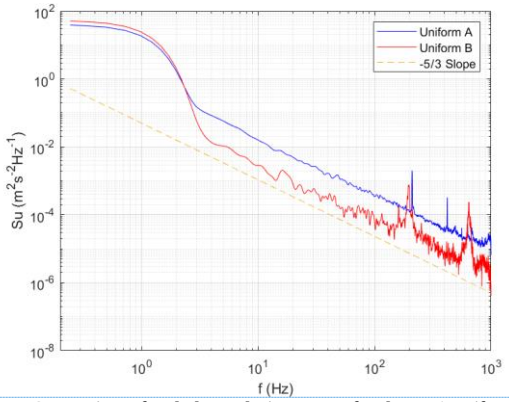

Figure 5. Comparison of turbulent velocity spectra for the 5 m/s uniform flow cases

3.4. Uncertainty analysis

The epistemic uncertainty of the cobra probes depends on turbulence levels~~,~~ but is generally within ±0.5 m/s ~~on average~~, up to about 30% turbulence intensity according to the manufacturer company (TFI Ltd., 2011). Considering the 5 m/s average wind velocity in the experiments the uncertainty of the probes is 10%. The JR3 multi-axis force/ torque sensor (~~75E20S1~~75E20S4~~-~~6000N) at the base of the tower has ±0.25% nominal accuracy of the measuring value for all axes. The uncertainly related to measuring and converting the analog voltages to digital for each signal is negligible.

All the values from the measuring instruments presented in section 4 have been filtered by moving average method except for the rotor speed. ~~The averaging window for wind velocities, generator voltage and load signals were chosen as 0.2, 0.2 and 0.5 second respectively, which preserve the main shape of signal by just filtering low powered high frequency fluctuations. Therefore, the RMS values for aleatoric uncertainty averaged in all the experiments in reading the cobra probes and power are ±0.48 m/s and ±0.04 W; the corresponding values for forces and moments in X, Y and Z axis are ±1.13 N, ±0.69 N, ±0.77 N ±1.52 Nm, ±3.17 Nm, ±0.31 Nm respectively. The combined uncertainties in percentage of their corresponding mean values are tabulated in Table 2. The large percentage error in some of the quantities are due to their very small corresponding average values~~The averaging window for the wind velocities, the generator voltage, and the loads were chosen as 0.2, 0.2, and 0.5 second respectively based on the criteria described in (Chowdhury et al., 2018), which preserved the main shape of signal time history filtering low powered high frequency fluctuations. Therefore, the processed data have aleatoric or random uncertainties within. The combined uncertainties then have been calculated with root sum squared of these two types of uncertainties and presented in percentage of their corresponding mean values in Table 2. The large amount of relative uncertainties in some of

Formatted: English (Canada)
Formatted: English (Canada)
Formatted: English (Canada)
Formatted: English (Canada)
Formatted: English (Canada)
Formatted: English (Canada)
Formatted: English (Canada)
Formatted: English (Canada)
Formatted: English (Canada)
Formatted: English (Canada)
Formatted: English (Canada)
Formatted: English (Canada)
Formatted: English (Canada)
Formatted: English (Canada)
Formatted: English (Canada)

the quantities are due to their very small corresponding average values (e.g. a fluctuating value around zero). The propagation of uncertainty due to normalizing some of the parameters in extreme operational cases with steady cases have been neglected.

Table 2. The combined uncertainty estimation of the measured values averaged in all the experiments

	Mean Values	Epistemic uncertainty	Aleatoric uncertainty	Combined uncertainty
Wind velocity	5 m/s	±10%	±9.60%	±13.86%
Power	0.70 W	±~ ± 0 %	±5.71%	±5.71%
X-force	14.37 N	±0.25%	±7.86%	±7.86%
Y-force	0.60 N	±0.25%	±114.12%	±114.12%
Z-force	4.99 N	±0.25%	±15.42%	±15.42%
X-moment	0.85 Nm	±0.25%	±178.21%	±178.21%
Y-moment	23.00 Nm	±0.25%	±13.78%	±13.78%
Z-moment	0.24 Nm	±0.25%	±125.54%	±125.54%

4. ~~Turbine test~~Test case results

4.1. Unsteady EWS

The time history of the results from EVS, negative EVS and EHS cases generated by changing the fan power set-points are presented in Figure 6a , b ~~and~~& c respectively. There are five windows (*I, II, III, IV & V*) in all of these sub-figures~~; the first~~ which have been arranged as follows: window ~~at the top~~*I* shows the filtered wind velocity time histories from the four cobra probes; ~~next~~ window *II* shows the normalized electrical power ~~performance~~ along with the TSR; ~~next three~~ windows *III*, *IV* and *V* show the filtered forces and moments time histories exerted at the tower base~~.~~ in X, Y and Z axes respectively. Note that in these figures, axes forces have been referred as shears, as they are shear forces at the base. The ~~stared~~starred axis indexes are normalized by their corresponding values from uniform case A. ~~The second~~In addition, a 10 seconds window around the extreme events has been four times magnified and replotted at the right sides of these sub figures which present the effect of extreme event in better details. The vertical red dashed line passes through the first wind velocity peak, and it has been assumed as the center of the event. Based on this line a 5 seconds red window has been depicted that highlights the theoretical duration of the extreme event in the magnified plots.

Window *II*, in all ~~the Figure 6a, b & c~~figures illustrates that these transient shear cases do not have a significant effect on the overall power performance of the wind turbine. The initial increase and decrease in power productions are just due to the time lag ~~(~1.5*s*)~~ between the high and the low peaks of the shears ~~hitting~~ (~1.5*s*) reaching the rotor which is noticeable from magnified cobra probes time history in the window *I* in Figure 6~~c~~.a, b & c. More detail about the extreme event velocity fields

Formatted: English (Canada)
Formatted
Formatted: English (Canada)
Inserted Cells
Formatted Table
Formatted: English (Canada)
Formatted: English (Canada)
Formatted: English (Canada)
Formatted: English (Canada)
Formatted: English (Canada)
Formatted: English (Canada)
Formatted: English (Canada)
Formatted: English (Canada)
Formatted: English (Canada)
Formatted: English (Canada)
Formatted: English (Canada)
Formatted: English (Canada)
Formatted: English (Canada)
Formatted: English (Canada)
Formatted: English (Canada)
Formatted: English (Canada)
Formatted: English (Canada)
Formatted
Formatted
Formatted
Formatted
Formatted
Formatted: English (Canada)
Formatted
Formatted: English (Canada)
Formatted
Formatted: English (Canada)

are accessible in (Shirzadeh et al., 2020). The EVSs do not have any significant effect on the loads at the base of the tower (windows *III*, *IV* & *V* in Figure 6a & b).

The ~~EVSs (Figure 6a & b) do not have any significant effect on the loads at the base of the tower either. These extreme shears could induce severe fatigue loads at the blade's bearing, blade's root, and the yaw bearing.~~highly correlated behaviour ~~Having load cells at the blades' roots and nacelle-tower junction or yaw bearing could have given more information about the loads' dynamics and the out-of-plane moment in these scenarios.~~

~~The correlation~~ between force in X axis and moment around Y axis is ~~clearly visible~~clear in all these figures~~.~~, comparing windows *III* & *IV*, The Y force shows random ~~dynamics~~fluctuations around zero with no correlation with ~~the~~other forces and moments. The Z force maintained the same value in these EWSs but shows no correlation with other loads. The X moment which represents both the vortex shedding and the torque on the generator has the strongest fluctuation compare to the Y and Z moments time histories. The Z moment in the two EVS cases is a small fluctuating value close to zero due to slight horizontal non-homogeneity of the flow-field. Theoretically, it should remain the same even at the time EVSs happen but as window *V* in Figure 6a & b demonstrate there are small variation in the Z moments which can be due to different efficiency of the fans in acceleration and deceleration.

Formatted: English (Canada)
Formatted: English (Canada)
Formatted: English (Canada)
Formatted: English (Canada)
Formatted: English (Canada)
Formatted: English (Canada)
Formatted: English (Canada)
Formatted: English (Canada)
Formatted: English (Canada)
Formatted: English (Canada)
Formatted: English (Canada)

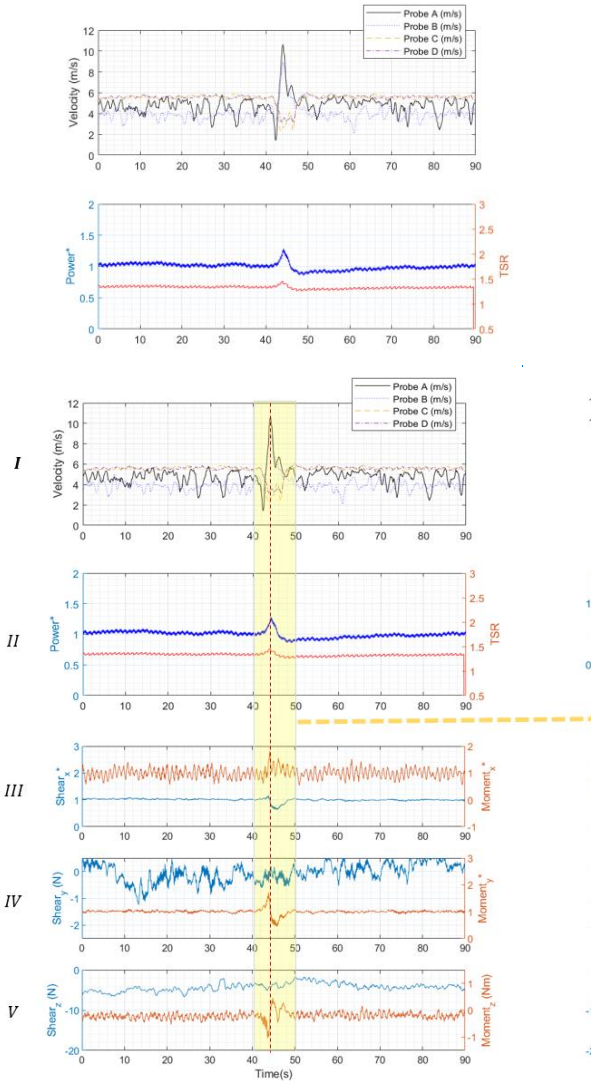

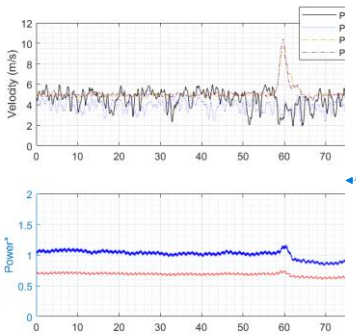

Formatted Table

Deleted Cells

Formatted: English (Canada)

Formatted: Indent: First line: 0.75 cm

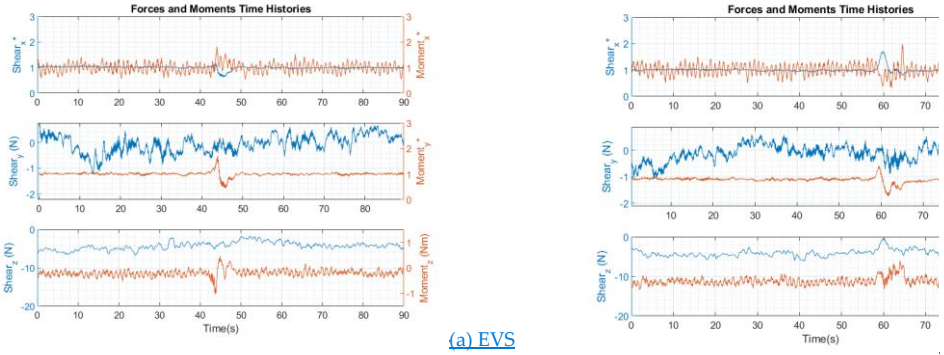

(a) EVS

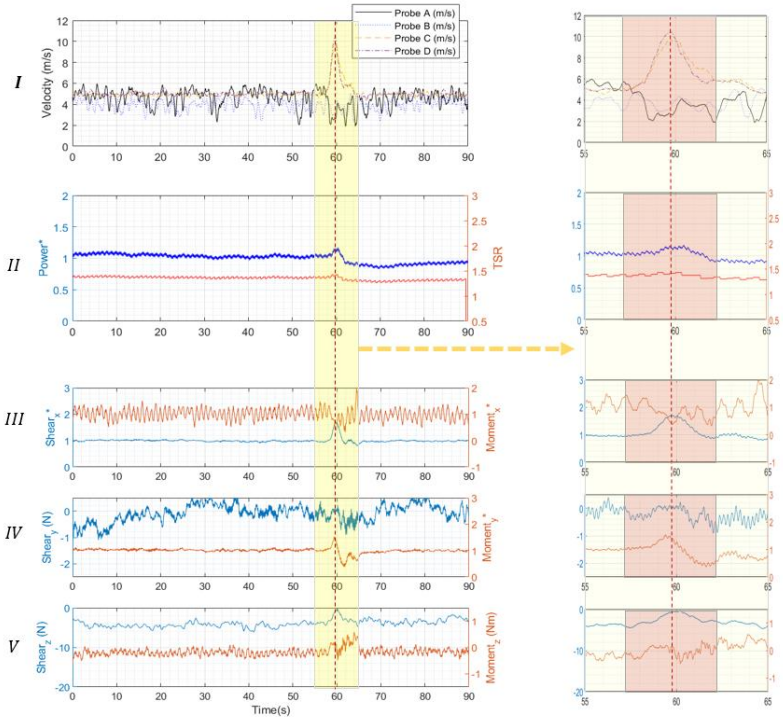

~~(a) EVS~~ (b) negative EVS

Formatted: English (Canada)

Deleted Cells

Formatted: English (Canada)

Formatted Table

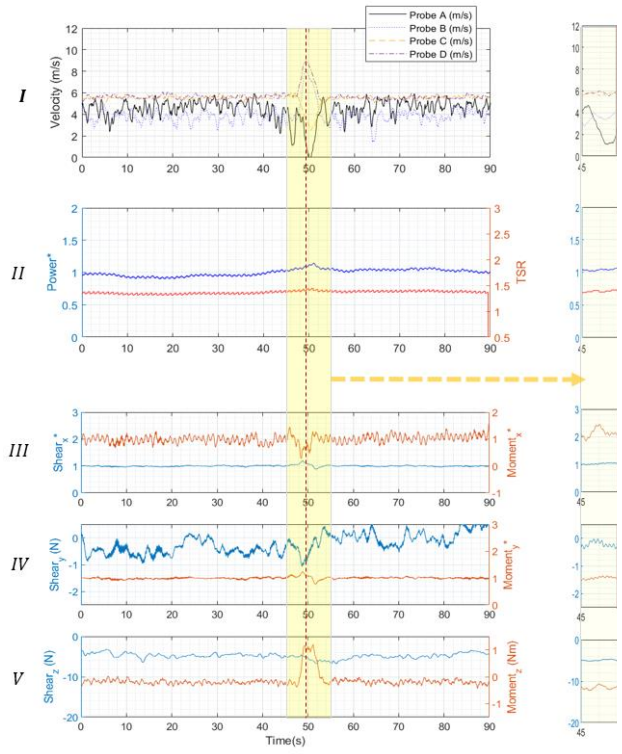

Formatted: English (Canada)

Formatted: English (Canada)

Deleted Cells

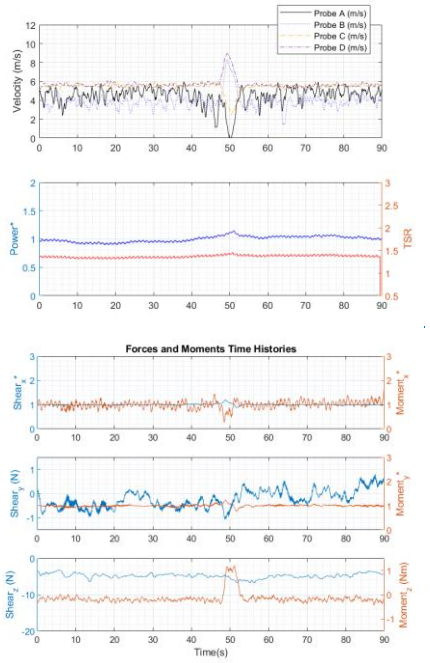

(c) EHS

Figure 6. The time history of the results from all the measuring instruments in (a) the EVS, (b) the negative EVS and (c) the EHS. ~~The five sub-figures in order~~Windows *I*, *II*, *III*, *IV* & *V* from top to bottom in each sub-figure show the wind velocities from 4 cobra probes, the power performance of the turbine, the X, the Y and the Z forces and moments at the base of the tower~~.~~, respectively. The ~~stared~~starred axis indexes are normalized by their corresponding value from uniform case A. 10 seconds window around the extreme events has been magnified and replotted at the right side of each sub-figure with a red 5 seconds window highliting the theorethical duration of the extreme event, and the red dashed line assumed as the center of the events which passes through the first velocity peak.

In the EHS case, the most important load component at the tower base ~~can be~~in terms of magnitude and its correlation with the extreme event is the Z axis moment. The ~~data~~window *V* in Figure 6c shows this extreme condition induces a 1.2 Nm ~~torsion~~yaw moment on the structure; normalizing this value using equation (9), yields 0.009414. For a full-scale wind turbine with ~~92m~~92 m diameter working in an average 10 m/s wind speed the induced yaw moment on the structure by an EHS event would be ~~351kNm~~351 kNm.

$$CM_z = \frac{M_z}{\frac{1}{2}\rho U^2 AD}. \quad (9)$$

~~ρ is the density of the air, A is the swept area of the rotor and D is the diameter.~~

Formatted: English (Canada)
Formatted Table
Formatted: English (Canada)
Formatted: English (Canada)
Formatted: English (Canada)
Formatted: English (Canada)
Formatted: English (Canada)
Formatted: English (Canada)
Formatted: English (Canada)
Formatted: English (Canada)
Formatted: English (Canada)
Formatted: English (Canada)
Formatted: English (Canada)
Formatted: English (Canada)
Formatted: English (Canada)
Formatted: English (Canada)
Formatted: English (Canada)
Formatted: English (Canada)
Formatted: English (Canada)
Formatted: English (Canada)
Formatted: English (Canada)
Formatted: English (Canada)
Formatted: English (Canada)
Formatted: English (Canada)
Formatted: English (Canada)
Formatted: English (Canada)
Formatted: English (Canada)
Formatted: English (Canada)
Formatted: English (Canada)
Formatted: English (Canada)
Formatted: English (Canada)
Formatted: English (Canada)
Formatted: English (Canada)
Formatted: English (Canada)
Formatted: English (Canada)
Formatted: English (Canada)

~~4.2. Unsteady EOG~~

where ρ is the density of the air, A is the swept area of the rotor and D is the diameter. As a full scale (87 m diameter) numerical simulation under steady velocity of 10 m/s with typical yaw condition suggests, the yaw moment can vary between ~ 30 to 90 kNm as the blades rotate (Cai et al., 2016). Accordingly, the amount of yaw moment induced by the EHS (varying between 0 to 350 kNm) is at least three times the magnitude of the yaw experienced by the turbine in uniform inflow conditions.

4.2. Unsteady EOG

The EOG ~~was generated using IGVs. As the time histories of the measuring instruments suggest this uniform gust has the most significant effect on both~~significantly affected the power generation and the loads. As the ~~second~~ window *II* in Figure 7 shows, this event can dangerously increase the rotor rotational speed ~~if no active or passive controlling~~without control systems ~~are being used~~ (the TSR ~~is changing from ~1 *to* 1.33).~~increased 33%). The electrical power increased 148% at the end of the gust event. ~~The~~However, the electrical power generation might not be the proper quantity for comparison at these low rotational speeds. The generator efficiency is highly dependent on the rotor speed. Therefore, some part of this ~~significant increase~~boost in power production is due to the ~~increase in~~fact that generator efficiency~~.~~ also increased as the rotor speeded up. The mechanical power should be a better quantity for comparison, ~~which is highly dependent on the operational TSR.~~but it was not possible to measure with the current setup. The ~~rotor will generate different amount of torque in different TSRs. Therefore, a similar gust on a similar wind turbine can have different effects in different operating TSRs. The same applies for the loads.~~

~~The~~ overall drag on the structure (X shear) and ~~the main~~its bending moment (Y moment) at the base, increased by 105% and 167 ~~%~~%, respectively. ~~Their difference depends on the hub height and the rotor diameter; in the current setup the average Y moment to the average X shear ratio is ~1.55.~~

Formatted: English (Canada)
Formatted: English (Canada)
Formatted: English (Canada)
Formatted: English (Canada)
Formatted: English (Canada)
Formatted: English (Canada)
Formatted: English (Canada)
Formatted: English (Canada)
Formatted: English (Canada)
Formatted: English (Canada)
Formatted: English (Canada)
Formatted: English (Canada)
Formatted: English (Canada)
Formatted: English (Canada)
Formatted: English (Canada)
Formatted: English (Canada)

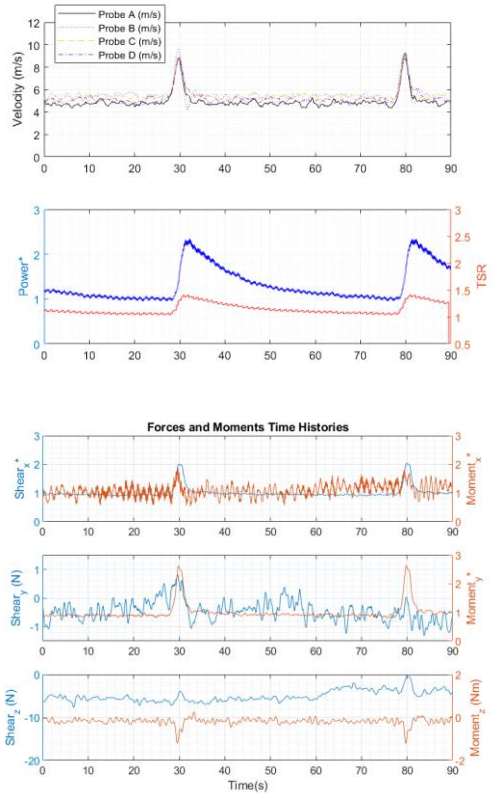

Figure 7. The time history of the results from all the probes in EOG using IGVs from top to bottom in order, the wind velocities from 4 cobra probes, power performance of the turbine, the forces and moments at the tower base, The stared axis indexes are normalized by their corresponding value from uniform case B

The loads usually have the same According to the magnified windows in Figure 7, the loads have similar profile shape as the gust with the same order of rising and falling time. (windows *III* & *IV*). Although, the power generation peak happens at the end of the gust event and then slowly decays afterwards. (window *II*). The extractable energy in a gust with a specific amplitude and time duration partially accumulates in the rotor rotational momentum with the residueexcess in form of higher instantaneous electrical power generation. After the gust event, the stored momentum slowly decays by transforminggradually transforms into electrical power as it can be seen in the second window of the Figure 7.

Formatted: English (Canada)
Formatted: English (Canada)
Formatted: English (Canada)
Formatted: English (Canada)
Formatted: English (Canada)
Formatted: English (Canada)
Formatted: English (Canada)
Formatted: English (Canada)
Formatted: English (Canada)

. The gust ~~affects the X moment contributed by~~abruptly increases the rotor torque. Therefore, ~~the~~it causes sudden increase in the ~~wind speed (gust) causes abrupt increase in the~~ X moment ~~which has~~with approximately ~~the same~~similar rising and falling time ~~as the gust. the~~to itself (window *III*). The Y shear/ force again has no ~~correlation with~~response to the gust. There is a slight correlation between Z force and the gust which ~~results~~can be interpreted as in a lift on the turbine (signal moves from negative values toward zero in the ~~last sub-figure in Figure 7).~~window *V*). Also, there is a rather large negative correlation between the Z moment and the gust. As the gust happens it pushes and tilts the rotor up which induces a gyroscope moment (~1.2 Nm) on the structure. Note that this highly depends on the ~~structure~~structural integrity of the wind turbine and might not happen in commercial HAWTs.

Formatted: English (Canada)
Formatted: English (Canada)
Formatted: English (Canada)
Formatted: English (Canada)
Formatted: English (Canada)
Formatted: English (Canada)
Formatted: English (Canada)
Formatted: English (Canada)
Formatted: English (Canada)
Formatted: English (Canada)
Formatted: English (Canada)

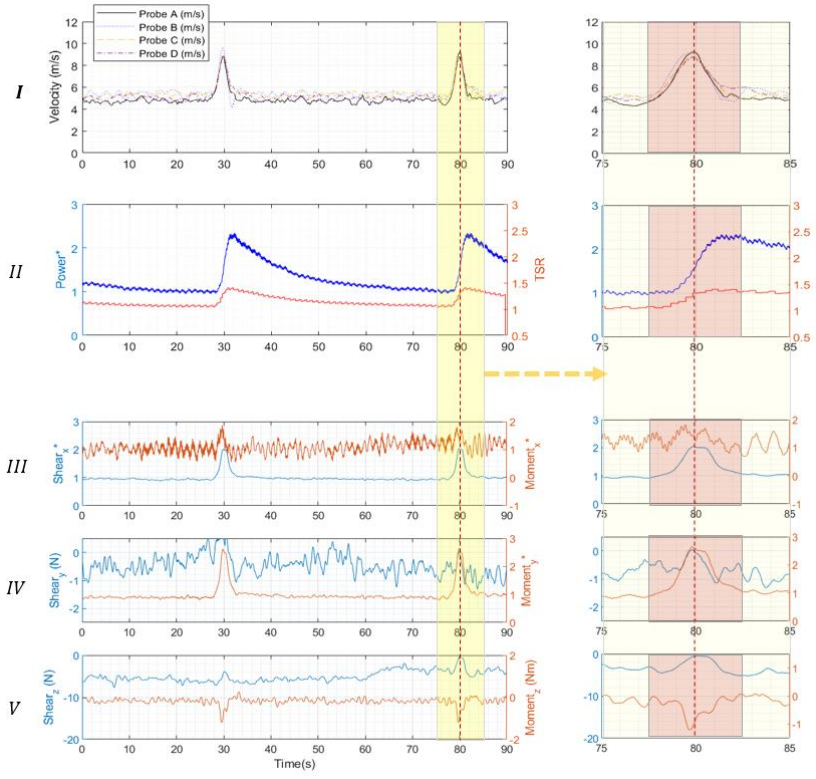

Figure 7. The time history of the results from all the probes in EOG using IGVs; Window *I*, the wind velocities from 4 cobra probes; Window *II*, power performance of the turbine, Windows *III*, *IV* & *V*, the forces and moments at the tower base; The starred axis indexes are normalized by their corresponding value from uniform case B. 10 seconds window around the extreme events has been magnified and replotted at the right side with a red 5 seconds window highliting the theorithical duration of the extreme event, and the red dashed line assumed as the center of the events which passes through the first velocity peak.

4.3. Reproducibility of the extreme events

In order to investigate the reproducibility of these extreme events in the WindEEE dome, a normalized cross correlation of the velocity signals, between the current and the previous study (Shirzadeh et al., 2020) has been performed. The reference probes from the previous study are probes H and B that were installed at similar heights or lateral distances depended on the event. For example, probe H in the EVS event was located at 3 m height in the previous study, similar the probes A and B in

this study. For the analysis, firstly, the velocity data in a 20 seconds window around the event has been extracted from both velocity time histories; secondly, with a specific amount of time lag between the velocity signals from this study and the reference probe, the extreme events were perfectly aligned; finally, the normalized cross correlation was calculated. This way, the shape of the velocity signals were compared. At the end, the averaged value of similarity from all the four probes has been reported as the overall similarity of these events to the previous study as it has been tabulated in Table 3. Accordingly, the IGVs are highly capable of generating similar profiles of EOG with more than 99% of similarities. Modulating the fan power set-points for creating the EHS and EVSs are showing consistent results with around 97% and 94% of similarities.

Table 3. The reproducibility analysis based on the probes H and B from the previous study (Shirzadeh et al., 2020)

Extreme event	Reference probe	Normalized cross-correlation		Overall similarity
EVS	Probe H	Probe A 91.89%	Probe B 93.19%	94.33%
	Probe B	Probe C 95.75%	Probe D 96.52%	
negative EVS	Probe H	Probe A 94.49%	Probe B 90.52%	95.10%
	Probe B	Probe C 97.65%	Probe D 97.77%	
EHS	Probe H	Probe B 96.48%	Probe D 98.47%	97.61%
	Probe B	Probe A 96.32%	Probe C 99.18%	
EOG	Probe H	Probe A 99.29%	Probe B 98.72%	99.17%
	Probe B	Probe C 99.26%	Probe D 99.43%	

Formatted: English (Canada)

5. Conclusions

An experimental study has been carried out to investigate the effect of transient extreme operating conditions based on the IEC standard (specifically EWSs and EOG) tailored and scaled for a 2.2 m diameter HAWT at the WindEEE dome at Western University. The main assumption used for the length and time scaling is that the duration of each extreme condition is equal to the ~~propagation~~advection time of the four tip vortex loops in the wake by the free stream. Other parameters were adjusted accordingly to accommodate for hardware limitations in generating the flow fields. Two uniform cases as the baselines for comparing the effect of different scenarios were also carried out.

The unsteady EVSs and EHS did not have any ~~significant~~noticeable effect on the power performance and overall loading at the base of the turbine. Nevertheless, EHS induced a significant yaw moment on the structure. These extreme shears could induce severe fatigue loads at the blades' bearings, blades' roots, and the yaw bearing. Having load cells at the blades' roots and nacelle-tower junction or yaw bearing could have given more information about the loads' dynamics and the out-of-plane moment in these scenarios. ~~noticeable torsion on the structure.~~

The EOG affects the turbine significantly. Results showed that ~~if no means of control for the rotor speed is considered~~ the power generation and loadings can increase significantly with a high dynamic behaviour. ~~Also, the reaction of the same wind turbine to the same EOG event can be different depending on the operational TSR.~~ In the EOG event, the loading profiles are corelated with the shape of the gust event itself (the peak of the loads are at the same point as the gust peak), but the power generation's peak happens at the end of the gust event.

Overall, this study presents an alternative experimental procedure for investigating the global loading and power generation of a ~~scaled~~ wind turbine under scaled reproducible deterministic transient wind conditions. The procedure has the potential to be improved and used for developing and testing new wind energy prototypes in transient conditions.

In future work, for the EVSs and EHS cases it is advisable to investigate the loads on the blades' roots and bearings as well as yaw bearing to implement a fatigue load analysis. In the present study the TSR was determined from wake effect scaling and physical limits of the test apparatus, resulting in a TSR~1.1. In future work, an attempt should be made to test at higher TSR through test apparatus and controller modifications. Testing of the effect of different extreme events durations at different operating TSRs would help validate the suggested time scaling.

Authors contributions

KS carried out all the experiments with supervision of HH. KS wrote the main body of the paper with input from all authors.

Competing interests

The authors declare that they have no conflict of interest

Formatted: English (Canada)
Formatted: English (Canada)
Formatted: English (Canada)
Formatted: English (Canada)
Formatted: English (Canada)
Formatted: English (Canada)
Formatted: English (Canada)
Formatted: English (Canada)
Formatted: English (Canada)
Formatted: English (Canada)
Formatted: English (Canada)

Acknowledgements

All authors thank Gerald Dafoe and Tristan Cormier for helping with the measurement setups. The present work is supported by the WindEEE dome CFI Grant and by NSERC Discovery Grant R2811A03.

References

Albers, A., Jakobi, T., Rohden, R. and Stoltenjohannes, J.: Influence of meteorological variables on measured wind turbine power curves, in European Wind Energy Conference and Exhibition 2007, EWEC 2007, vol. 3., 2007.

Anvari, M., Lohmann, G., Wächter, M., Milan, P., Lorenz, E., Heinemann, D., Tabar, M. R. R. and Peinke, J.: Short term fluctuations of wind and solar power systems, New ~~J. Phys.,~~Journal of Physics, 18(6), 063027, doi:10.1088/1367-2630/18/6/063027, 2016.

Bossanyi, E. A., Kumar, A. and Hugues-Salas, O.: Wind turbine control applications of turbine-mounted LIDAR, ~~J. Phys. Conf. Ser., vol.~~in Journal of Physics: Conference Series, vol. 555, Institute of Physics Publishing., 2014.

Burton, T., Jenkins, N., Sharpe, D. and Bossanyi, E.: Wind Energy Handbook, 2nd ed., John Wiley and Sons Ltd, Chichester, UK., 2011.

Cai, X., Gu, R., Pan, P. and Zhu, J.: Unsteady aerodynamics simulation of a full-scale horizontal axis wind turbine using CFD methodology, Energy Conversion and Management, 112, 146–156, doi:https://doi.org/10.1016/j.enconman.2015.12.084, 2016.

Chowdhury, J., Chowdhury, J., Parvu, D., Karami, M. and Hangan, H.: Wind flow characteristics of a model downburst, in American Society of Mechanical Engineers, Fluids Engineering Division (Publication) FEDSM, vol. 1, American Society of Mechanical Engineers (ASME)., 2018.

Feng, Y., Qiu, Y., Crabtree, C. J., Long, H. and Tavner, P. J.: Monitoring wind turbine gearboxes, Wind Energy, 16(5), 728–740, doi:10.1002/we.1521, 2013.

Hangan, H., Refan, M., Jubayer, C., Romanic, D., Parvu, D., LoTufo, J. and Costache, A.: Novel techniques in wind engineering, ~~J. Wind Eng. Ind. Aerodyn.,~~Journal of Wind Engineering and Industrial Aerodynamics, 171, 12–33, doi:10.1016/j.jweia.2017.09.010, 2017.

IEC: (International Electrotechnical Commission) IEC 61400-1: Wind turbines - Part 1: Design requirements, 3rd ed., Geneva, Switzerland., 2005.

IEC: (International Electrotechnical Commission) IEC 61400-1: Wind energy generation systems - Part 1: Design requirements, 4th ed., Geneva, Switzerland., 2019.

Li, L., Hearst, R. J., Ferreira, M. A. and Ganapathisubramani, B.: The near-field of a lab-scale wind turbine in tailored turbulent shear flows, ~~Renew.~~Renewable Energy, 149, 735–748, doi:https://doi.org/10.1016/j.renene.2019.12.049, 2020.

McKinsey & Company: Global Energy Perspective 2019 : Reference Case, Energy Insights, (January), 31, 2019.

Milan, P., Wächter, M. and Peinke, J.: Turbulent Character of Wind Energy, ~~Phys. Rev. Lett.,~~Physical Review Letters,

Formatted: English (Canada)

110(13), 138701, doi:10.1103/PhysRevLett.110.138701, 2013.

Petrović, V., Berger, F., Neuhaus, L., Hölling, M. and Kühn, M.: Wind tunnel setup for experimental validation of wind turbine control concepts under tailor-made reproducible wind conditions, ~~J. Phys. Conf. Ser., vol.~~ Journal of Physics: Conference Series, 1222~~.~~, 012013, doi:10.1088/1742-6596/1222/1/012013, 2019.

Pope, S. B.: Turbulent scalar mixing processes, Cambridge University Press., 2000.

Refan, M. and Hangan, H.: Aerodynamic Performance of a Small Horizontal Axis Wind Turbine, Journal of Solar Energy Engineering, 134(2), doi:10.1115/1.4005751, 2012.

Rezaeiha, A., Pereira, R. and Kotsonis, M.: Fluctuations of angle of attack and lift coefficient and the resultant fatigue loads for a large Horizontal Axis Wind turbine, , doi:10.1016/j.renene.2017.07.101, 2017.

Schottler, J., Reinke, N., Hölling, A., Whale, J., Peinke, J. and Hölling, M.: On the impact of non-Gaussian wind statistics on wind turbines – an experimental approach, Wind Energy ~~Sci.,~~Science, 2(1), doi:10.5194/wes-2-1-2017, 2017.

Sezer-Uzol, N. and Uzol, O.: Effect of steady and transient wind shear on the wake structure and performance of a horizontal axis wind turbine rotor, Wind Energy, 16(1), 1–17, doi:10.1002/we.514, 2013.

Shirzadeh, K., Hangan, H. and Crawford, C.: ~~Numerical and~~ Experimental ~~Simulation~~and numerical simulation of ~~Extreme Operational Conditions~~extreme operational conditions for ~~Horizontal Axis Wind Turbines Based~~horizontal axis wind turbines based on the IEC ~~Standard, Wind Energ. Sci. Discuss.,~~standard, Wind Energy Science, 5(4), 1755–1770, doi:10.5194/wes-5-1755-2020, 2020.

TFI Ltd.: Cobra Probe, ~~Turbul.~~Turbulent Flow ~~Instrum.~~Instrumentation Pty Ltd [online] Available from: https://www.turbulentflow.com.au/Products/CobraProbe/CobraProbe.php (Accessed 12 June 2020), 2011.

Wächter, M., Heißelmann, H., Hölling, M., Morales, A., Milan, P., Mücke, T., Peinke, J., Reinke, N. and Rinn, P.: The turbulent nature of the atmospheric boundary layer and its impact on the wind energy conversion process, ~~J. Turbul.,~~Journal of Turbulence, 13, doi:10.1080/14685248.2012.696118, 2012.

Wester, T. T. B., Kampers, G., Gülker, G., Peinke, J., Cordes, U., Tropea, C. and Hölling, M.: High speed PIV measurements of an adaptive camber airfoil under highly gusty inflow conditions, ~~J. Phys. Conf. Ser.,~~Journal of Physics: Conference Series, 1037, 072007, doi:10.1088/1742-6596/1037/7/072007, 2018.

Formatted: English (Canada)